

University of Wollongong
Research Online

Australian Institute for Innovative Materials -
Papers

Australian Institute for Innovative Materials

1-1-2013

Substitution of Y for Pr in PrMn_2Ge_2 -The magnetism of $\text{Pr}_{0.8}\text{Y}_{0.2}\text{Mn}_2\text{Ge}_2$

Jianli Wang

University of Wollongong, jianli@uow.edu.au

S J. Campbell

University of New South Wales

M Hofmann

Technische Universitat Munchen

S J. Kennedy

ANSTO

M Avdeev

ANSTO

See next page for additional authors

Follow this and additional works at: <https://ro.uow.edu.au/aiimpapers>



Part of the [Engineering Commons](#), and the [Physical Sciences and Mathematics Commons](#)

Recommended Citation

Wang, Jianli; Campbell, S J.; Hofmann, M; Kennedy, S J.; Avdeev, M; Md Din, M F.; Zeng, R; Cheng, Z X.; and Dou, S X., "Substitution of Y for Pr in PrMn_2Ge_2 -The magnetism of $\text{Pr}_{0.8}\text{Y}_{0.2}\text{Mn}_2\text{Ge}_2$ " (2013). *Australian Institute for Innovative Materials - Papers*. 696.

<https://ro.uow.edu.au/aiimpapers/696>

Research Online is the open access institutional repository for the University of Wollongong. For further information contact the UOW Library: research-pubs@uow.edu.au

Substitution of Y for Pr in PrMn₂Ge₂-The magnetism of Pr_{0.8}Y_{0.2}Mn₂Ge₂

Abstract

Pr_{0.8}Y_{0.2}Mn₂Ge₂ is found to exhibit four magnetic transitions on decreasing the temperature from the paramagnetic region: (i) paramagnetism to intralayer antiferromagnetism (AFI) at T_N intra; (ii) AFI to canted ferromagnetism (Fmc) at T_C inter; (iii) Fmc to conical magnetic ordering of the Mn sublattice (Fmi) at T_{cc}; and (iv) Fmi(Mn) to Fmi(Mn) + F(Pr) at T_C Pr. These changes in magnetic structure are discussed in terms of changes in the Mn-Mn separation distances caused by the unit cell contraction and by electronic effects due to replacement of 20% of Pr with Y.

Keywords

8y0, pr0, magnetism, 2mn2ge2, prmn2ge2, substitution, pr, y

Disciplines

Engineering | Physical Sciences and Mathematics

Publication Details

Wang, J., Campbell, S. J., Hofmann, M., Kennedy, S. J., Avdeev, M., Md Din, M. F., Zeng, R., Cheng, Z. & Dou, S. X. (2013). Substitution of y for Pr in PrMn₂Ge₂-The magnetism of Pr_{0.8}Y_{0.2}Mn₂Ge₂. *Journal of Applied Physics*, 113 (17), 17E147-1-17E147-3.

Authors

Jianli Wang, S J. Campbell, M Hofmann, S J. Kennedy, M Avdeev, M F. Md Din, R Zeng, Z X. Cheng, and S X. Dou

Substitution of Y for Pr in PrMn_2Ge_2 —The magnetism of $\text{Pr}_{0.8}\text{Y}_{0.2}\text{Mn}_2\text{Ge}_2$

J. L. Wang, S. J. Campbell, M. Hofmann, S. J. Kennedy, M. Avdeev et al.

Citation: *J. Appl. Phys.* **113**, 17E147 (2013); doi: 10.1063/1.4798622

View online: <http://dx.doi.org/10.1063/1.4798622>

View Table of Contents: <http://jap.aip.org/resource/1/JAPIAU/v113/i17>

Published by the [American Institute of Physics](#).

Additional information on *J. Appl. Phys.*

Journal Homepage: <http://jap.aip.org/>

Journal Information: http://jap.aip.org/about/about_the_journal

Top downloads: http://jap.aip.org/features/most_downloaded

Information for Authors: <http://jap.aip.org/authors>

ADVERTISEMENT



The advertisement banner features a green and yellow background with abstract wavy lines. On the left, the text "AIPAdvances" is displayed in a stylized font, with "AIP" in blue and "Advances" in green, accompanied by a series of orange dots of varying sizes. On the right, a circular seal contains the text "Now Indexed in Thomson Reuters Databases". Below this, a blue horizontal bar contains the text "Explore AIP's open access journal:". To the right of this bar, a list of three bullet points is shown: "• Rapid publication", "• Article-level metrics", and "• Post-publication rating and commenting".

AIPAdvances

Now Indexed in
Thomson Reuters
Databases

Explore AIP's open access journal:

- Rapid publication
- Article-level metrics
- Post-publication rating and commenting

Substitution of Y for Pr in PrMn_2Ge_2 —The magnetism of $\text{Pr}_{0.8}\text{Y}_{0.2}\text{Mn}_2\text{Ge}_2$

J. L. Wang,^{1,2,3,a)} S. J. Campbell,³ M. Hofmann,⁴ S. J. Kennedy,² M. Avdeev,² M. F. Md Din,¹ R. Zeng,¹ Z. X. Cheng,¹ and S. X. Dou¹

¹*Institute for Superconductivity and Electronic Materials, University of Wollongong, Wollongong, NSW 2522, Australia*

²*Bragg Institute, ANSTO, Lucas Heights, NSW 2234, Australia*

³*School of Physical, Environmental and Mathematical Sciences, The University of New South Wales, Canberra, ACT 2600, Australia*

⁴*FRM-II, Technische Universität München, 85747 Garching, Germany*

(Presented 18 January 2013; received 23 October 2012; accepted 4 January 2013; published online 8 April 2013)

$\text{Pr}_{0.8}\text{Y}_{0.2}\text{Mn}_2\text{Ge}_2$ is found to exhibit four magnetic transitions on decreasing the temperature from the paramagnetic region: (i) paramagnetism to intralayer antiferromagnetism (AFI) at T_N^{intra} ; (ii) AFI to canted ferromagnetism (Fmc) at T_C^{inter} ; (iii) Fmc to conical magnetic ordering of the Mn sublattice (Fmi) at T_{CC} ; and (iv) Fmi(Mn) to Fmi(Mn) + F(Pr) at T_C^{Pr} . These changes in magnetic structure are discussed in terms of changes in the Mn-Mn separation distances caused by the unit cell contraction and by electronic effects due to replacement of 20% of Pr with Y. © 2013 American Institute of Physics. [<http://dx.doi.org/10.1063/1.4798622>]

Studies of materials that exhibit a large magnetocaloric effect (MCE) and potential for applications in magnetic refrigeration are important as sustainable and environmentally friendly alternatives to current refrigeration technologies [e.g., Ref. 1]. The discovery of a giant MCE in $\text{Gd}_5(\text{Si}_2\text{Ge}_2)$ (Ref. 2) led to increased efforts in the search for materials with a large MCE. The tetragonal intermetallic compounds RT_2X_2 (R = rare-earth; T = transition metal, and X = Si or Ge), with a layered structure similar to that of the $\text{Gd}_5\text{Si}_2\text{Ge}_2$ system, exhibit a wide range of magnetic behaviours and have been studied extensively in the continuing searching for novel MCE materials.^{3–5} Among them, PrMn_2Ge_2 and related compounds offer interesting prospects for enhanced magnetocaloric behaviour⁶ as their layered structure allows control of the intrinsic magnetism of the Mn sublattice via inter-planar and intra-planar separations of the Mn atoms with the Pr atoms contributing to increased magnetization due to ferromagnetic coupling between the Mn and Pr sublattices below the Pr ordering temperature T_C^{Pr} .⁶ Based on the smaller atomic radius of Y (=1.78 Å) compared with Pr (1.82 Å), substitution of Y for Pr in PrMn_2Ge_2 is expected to lead to a significant decrease in $d_{\text{Mn-Mn}}$ and a corresponding drastic modification of magnetic states.^{7,8} Here, we outline the influence of substituting Pr with Y in $\text{Pr}_{1-x}\text{Y}_x\text{Mn}_2\text{Ge}_2$ with $x = 0.0$ – 1.0 and present a detailed determination of the intrinsic magnetism of $\text{Pr}_{1-x}\text{Y}_x\text{Mn}_2\text{Ge}_2$ with $x = 0.2$.

The $\text{Pr}_{1-x}\text{Y}_x\text{Mn}_2\text{Ge}_2$ (with $x = 0.0$ – 1.0) samples were prepared by arc melting stoichiometric amounts of the pure elements and then sealed under vacuum in a quartz tube, annealed for 1 week at 900 °C, and quenched in water. Neutron diffraction experiments were carried out on the GEM time-of-flight diffractometer at ISIS (STFC, UK) from 30 to 360 K (Ref. 8) and the Echidna diffractometer at OPAL.

Cu-K α x-ray diffraction confirmed that the $\text{Pr}_{1-x}\text{Y}_x\text{Mn}_2\text{Ge}_2$ compounds crystallize in the tetragonal ThCr_2Si_2 -structure and

that the lattice parameters decrease as the Y concentration increases as expected, with the change in unit cell volume for $\text{Pr}_{1-x}\text{Y}_x\text{Mn}_2\text{Ge}_2$ given by $dV/dx \sim -12.4 \text{ Å}^3$ ($da/dx \sim -0.131 \text{ Å}$ and $dc/dx \sim -0.053 \text{ Å}$). The overall magnetic behaviour of RMn_2Ge_2 compounds is strongly influenced by two critical intralayer Mn–Mn distances $d_{\text{Mn-Mn}}^{\text{intra}}$: $d_{\text{crit1}} = 2.87 \text{ Å}$ and $d_{\text{crit2}} = 2.84 \text{ Å}$.^{3–6} It has been found that for $\text{Pr}_{1-x}\text{Y}_x\text{Mn}_2\text{Ge}_2$ compounds the Mn–Mn intralayer distance $d_{\text{Mn-Mn}}^{\text{intra}}$ decreases significantly with increasing Y content from 2.915 Å for $x = 0$ ($> d_{\text{crit1}}$) to 2.826 Å for $x = 1.0$ ($< d_{\text{crit2}}$). The decrease in $d_{\text{Mn-Mn}}^{\text{intra}}$ is correspondingly accompanied with a change in the magnetic state at room temperature from ferromagnetism for $x < 0.7$ to antiferromagnetism for $x \geq 0.8$.^{7,8} Refinement of the room temperature neutron diffraction pattern of $\text{Pr}_{0.8}\text{Y}_{0.2}\text{Mn}_2\text{Ge}_2$ yields the intralayer Mn–Mn spacing $d_{\text{Mn-Mn}}^{\text{intra}} = 2.907 \text{ Å} > d_{\text{crit1}} = 2.87 \text{ Å}$.

The temperature dependence of the magnetization ($H = 100 \text{ Oe}$; 10–340 K) and DSC results (300–600 K) for $\text{Pr}_{0.8}\text{Y}_{0.2}\text{Mn}_2\text{Ge}_2$ are shown as a composite figure in Fig. 1. Four magnetic transitions (rather than one as reported in Ref. 7) can be readily identified for $\text{Pr}_{0.8}\text{Y}_{0.2}\text{Mn}_2\text{Ge}_2$ with transition temperatures $T_N^{\text{intra}} = 375 \text{ K}$, $T_C^{\text{inter}} = 335 \text{ K}$, $T_{CC} = 245 \text{ K}$, and $T_C^{\text{Pr}} = 42 \text{ K}$ as discussed below (the transition temperatures T_C^{inter} , T_N^{intra} , and T_C^{Pr} were defined as the temperatures at which dM/dT diverges⁹). The M-T data were measured in a field of 100 Oe over the temperature range of 10–340 K after cooling in zero field (the warming and cooling curves are marked by arrows) with magneto-history effects evident at $T_C^{\text{inter}} = 335 \text{ K}$.¹⁰ Magnetization measurements at 10 K, 50 K, and 250 K in fields up to 5 T yield a saturation magnetization of 45.0 emu/g (3.11 $\mu_B/\text{f.u.}$), 38.2 emu/g (2.64 $\mu_B/\text{f.u.}$), and 35.9 emu/g (2.48 $\mu_B/\text{f.u.}$), respectively, indicating substantial FM order. Based on the analogous magnetic behaviour between PrMn_2Ge_2 (Ref. 3) and $\text{Pr}_{0.8}\text{Y}_{0.2}\text{Mn}_2\text{Ge}_2$ and the neutron refinements described below, in order of decreasing temperature, the four transition temperatures can be defined as T_N^{intra} , T_C^{inter} , T_{CC} , and T_C^{Pr} .

Fig. 2(a) shows a representative set of neutron diffraction patterns for $\text{Pr}_{0.8}\text{Y}_{0.2}\text{Mn}_2\text{Ge}_2$ at 10 K steps over the

^{a)}Author to whom correspondence should be addressed. Electronic mail: jianli@uow.edu.au.

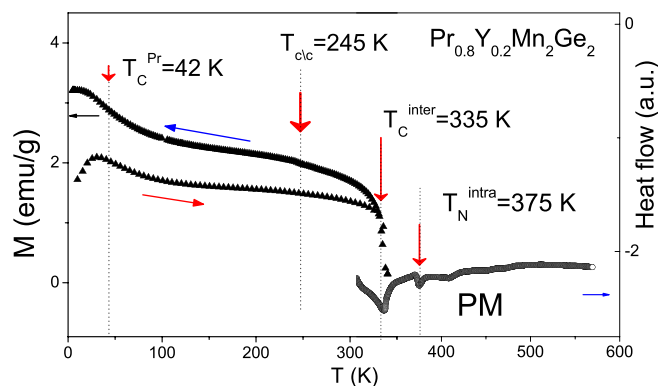


FIG. 1. Composite figure showing the temperature dependent magnetization obtained on cooling $\text{Pr}_{0.8}\text{Y}_{0.2}\text{Mn}_2\text{Ge}_2$ in a field of 100 Oe (left part; 10–340 K) and the differential scanning calorimetry results (right part; 300–600 K). The M-T curves show the results for warming and then cooling after first cooling from room temperature in zero field (transition temperatures indicated by arrows).

temperature range of 30–360 K. As described elsewhere [e.g., Ref. 3], the temperature dependences of the intensities of the (112), (101), and (103) peaks (Fig. 2(b)) correspond well with changes in magnetic states at $T_{\text{C}}^{\text{inter}}$, T_{C}^{cc} , and T_{C}^{Pr} as indicated by the magnetic studies (Fig. 1) as discussed above. Fig. 2(c) shows a series of neutron diffraction patterns and Rietveld refinements of $\text{Pr}_{0.8}\text{Y}_{0.2}\text{Mn}_2\text{Ge}_2$ at selected temperatures. These patterns exemplify the four different magnetic regions and structures encountered below

$T_{\text{N}}^{\text{intra}} = 375$ K. Here, we describe the magnetic structures in terms of the notation outlined by Venturini *et al.*¹⁰

The first magnetic transition occurs around $T_{\text{N}}^{\text{intra}} \sim 375$ K. While we were unable to collect diffraction patterns above ~ 360 K during the experiments at ISIS,⁸ refinements of the neutron patterns between 360 K and 335 K confirmed that the compound exhibits the AFI magnetic structure (this is reflected, for example, by the increase in the (101) peak intensity as in Figs. 2(a) and 2(b)). This allows us to ascribe the transition temperature $T_{\text{N}}^{\text{intra}} \sim 375$ K as originating from the transition from paramagnetism to intralayer antiferromagnetism (AFI).

The second transition at $T_{\text{C}}^{\text{inter}} \sim 335$ K is clearly reflected by enhancements of both the (112) and (101) peak as the temperature decreases (Figs. 2(a)–2(c)). This behaviour indicates the presence of components of the Mn moment below 335 K both within the ab-plane (AF order as reflected by the (101) peak) and along the c-axis (FM order as indicated by the (112) peak). It is therefore concluded that the transition at $T_{\text{C}}^{\text{inter}} = 335$ K reflects the change from the AFI magnetic structure to the canted ferromagnetic spin structure Fmc.

The onset of satellite reflections $(101)^+$, $(101)^-$, $(103)^+$, and $(103)^-$ at $T_{\text{C}}^{\text{cc}} \sim 245$ K mark formation of the conical configuration Fmi magnetic state (see Figs. 2(a) and 2(c)). The Fmi structure represents the ferromagnetic mixed incommensurate structure characterised by ferromagnetic interplanar coupling of the in-plane ferromagnetic

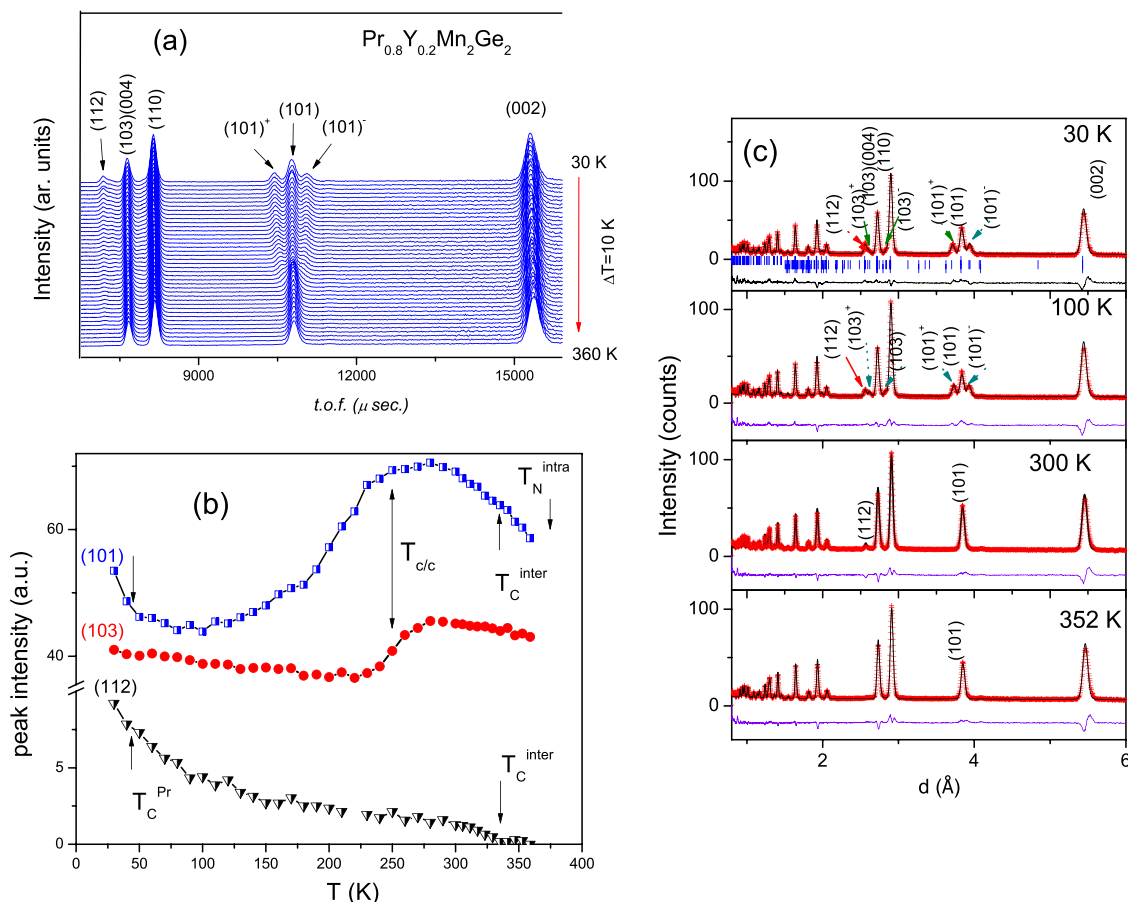


FIG. 2. (a) Representative neutron diffraction patterns for $\text{Pr}_{0.8}\text{Y}_{0.2}\text{Mn}_2\text{Ge}_2$ at 10 K intervals over the temperature range of 30–360 K (GEM, ISIS, STFC); (b) temperature dependences of the (101), (103), and (112) peak intensities; (c) neutron diffraction patterns of $\text{Pr}_{0.8}\text{Y}_{0.2}\text{Mn}_2\text{Ge}_2$ at 30 K, 100 K, 300 K, and 352 K. The full lines through the data represent the Rietveld refinements with the differences plot also shown for each pattern and refinement.

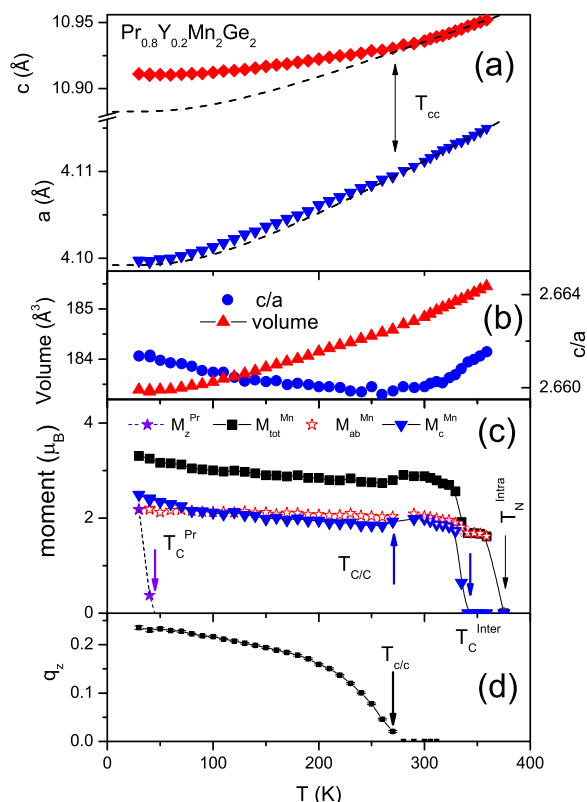


FIG. 3. Temperature dependences of structural and magnetic parameters for $\text{Pr}_{0.8}\text{Y}_{0.2}\text{Mn}_2\text{Ge}_2$ as derived from refinements of the neutron diffraction patterns. (a) Lattice parameters a , c ; (b) unit cell volume c/a ; (c) magnetic moment; (d) the q_z component of the wavevector. The dashed lines in Fig. 3(a) show the phonon contribution to the lattice expansion as evaluated from the Grüneisen relation.

components and by the incommensurate arrangement of the antiferromagnetic in-plane components. The component q_z of the wavevector dictates the phase difference between Mn spin along the screw axis \mathbf{c} equal to $2\pi(0, 0, q_z)(0, 0, 1) = 2\pi q_z$.³ The temperature dependence of the propagation vectors q_z has been derived from the Rietveld refinements and is presented in Fig. 3(d).

Further increases in the intensities of both the (112) and (101) peak are observed on cooling $\text{Pr}_{0.8}\text{Y}_{0.2}\text{Mn}_2\text{Ge}_2$ below $T_C^{\text{Pr}} \sim 42$ K (Fig. 2(b)). As supported by refinements of the neutron patterns, this additional magnetic scattering is due to ferromagnetic ordering of the Pr magnetic sublattice, F(Pr), leading to a combination of the Fmi structure of Mn-sublattice and the ferromagnetic ordering of the Pr magnetic sublattice F(Pr) below $T_C^{\text{Pr}} \sim 42$ K. At 30 K, it has been derived that the Pr and Mn magnetic moments are $2.18 \mu_B$ and $3.31 \mu_B$, respectively, with $q_z = 0.235$. The canting angle of Mn moments with respect to the c -axis at 30 K is derived to be 41.2° . Compared with q_z in PrMn_2Ge_2 compound ($q_z = 0.28$ at 2 K) and $\text{Pr}_{0.8}\text{Lu}_{0.2}\text{Mn}_2\text{Ge}_2$ ($q_z = 0.21$ at 3 K),³ it can be seen that the replacement of the nonmagnetic elements Y or Lu for Pr leads to a decrease in q_z and that Lu is more effective than Y in modifying q_z .

The structural and magnetic moment values resulting from refinements of the variable temperature neutron diffraction data (~ 30 – 360 K) are shown in Fig. 3. The unit cell is found to exhibit an anisotropic change with increasing

temperature (e.g., c/a versus T graph of Fig. 3(b)) with a pronounced magneto-volume effect evident (especially in the c -axis). The dashed lines in Fig. 3(a) show the phonon contribution to the lattice expansion as evaluated from the Grüneisen relation using a Debye temperature $\theta_D = 400$ K [see Ref. 4] and extrapolated from the paramagnetic region into the magnetically ordered region for comparison with the experimental lattice parameters.¹¹

Compared with the transition temperatures reported for PrMn_2Ge_2 ($T_N^{\text{intra}} = 415$ K, $T_C^{\text{inter}} = 334$ K, $T_{\text{cc}} = 280$ K, and $T_C^{\text{Pr}} = 100$ K),¹² replacement of Pr with 20% of Y leads to a reduction in the transition temperatures (other than T_C^{inter} which remains essentially unchanged). Given that contraction of the unit cell volume due to Y substitution (chemical pressure) can be considered equivalent to the influence of external pressure, the corresponding chemical pressure can be derived to be 5.0 kbar for $\text{Pr}_{0.8}\text{Y}_{0.2}\text{Mn}_2\text{Ge}_2$ using the Murnaghan equation.³ Using the values of $dT_C^{\text{Pr}}/dp = -5.8$ K/kbar for $\text{Pr}_{0.5}\text{Y}_{0.5}\text{Mn}_2\text{Ge}_2$ compound¹³ and $dT_C^{\text{inter}}/dp = -0.2$ K/kbar for PrMn_2Ge_2 ,¹⁴ the expected values of T_C^{Pr} and T_C^{inter} due to the “chemical pressure” in $\text{Pr}_{0.8}\text{Y}_{0.2}\text{Mn}_2\text{Ge}_2$ should be $T_C^{\text{Pr}} = 71$ K and $T_C^{\text{inter}} = 333$ K. Compared with the experimental values of $T_C^{\text{Pr}} = 42$ K and $T_C^{\text{inter}} = 335$ K in $\text{Pr}_{0.8}\text{Y}_{0.2}\text{Mn}_2\text{Ge}_2$, it can be concluded that in addition to the geometric effects associated with the interplanar and intra-planar separation distances as discussed above, changes in the electronic configurations due to Y substitution for Pr as well as increase in the concentration of the nonmagnetic Y atoms, have a significant effect on the overall magnetic behaviour of $\text{Pr}_{0.8}\text{Y}_{0.2}\text{Mn}_2\text{Ge}_2$.

$\text{Pr}_{0.8}\text{Y}_{0.2}\text{Mn}_2\text{Ge}_2$ compound follows the sequence of magnetic structures with decreasing temperature: PM \rightarrow AFI \rightarrow Fmc \rightarrow Fmi \rightarrow Fmi + F(Pr). Replacement of Pr with 20% of Y leads to a reduction in the transition temperatures and the q_z propagation vector component compared with the behaviour shown by PrMn_2Ge_2 .

This work was supported in part by Australian Research Council (DP110102386). The work was also supported by the Access to Major Research Facilities Program. J.L.W., S.J.C., and M.H. acknowledge the assistance of Professor P. Radaelli during experiments carried out at GEM, ISIS, and STFC.

¹E. Brück, *J. Phys. D: Appl. Phys.* **38**, R381 (2005).

²V. K. Pecharsky and K. A. Gschneidner, Jr., *Phys. Rev. Lett.* **78**, 4494 (1997).

³J. L. Wang *et al.*, *J. Appl. Phys.* **104**, 103911 (2008); J. L. Wang *et al.*, *J. Phys.: Condens. Matter* **21**, 124217 (2009).

⁴J. L. Wang *et al.*, *Appl. Phys. Lett.* **98**, 232509 (2011).

⁵L. Li, K. Nishimura *et al.*, *Appl. Phys. Lett.* **100**, 152403 (2012).

⁶J. L. Wang *et al.*, *J. Appl. Phys.* **105**, 07A909 (2009); R. Zeng *et al.*, *J. Alloys Compd.* **509**, L119 (2011).

⁷Y. G. Wang *et al.*, *J. Phys.: Condens. Matter* **9**, 8539 (1997).

⁸J. L. Wang *et al.*, “Magnetic structures in $\text{Pr}_{1-x}\text{Y}_x\text{Mn}_2\text{Ge}_2$ ” (unpublished).

⁹J. L. Wang *et al.*, *Phys. Rev. B* **67**, 014417 (2003).

¹⁰G. Venturini *et al.*, *J. Magn. Magn. Mater.* **150**, 197 (1995).

¹¹J. L. Wang *et al.*, *Phys. Rev. B* **75**, 174423 (2007).

¹²R. Welter *et al.*, *J. Alloys Compd.* **218**, 204 (1995).

¹³J. L. Wang *et al.*, “Driving magnetostructural transitions in layered intermetallic compounds,” *Phys. Rev. Lett.* (submitted).

¹⁴T. Kawashima *et al.*, *J. Magn. Magn. Mater.* **90–91**, 721 (1990).